IJST, Transactions of Mechanical Engineering, Vol. 37, No. M2, pp 161-174
Printed in The Islamic Republic of Iran, 2013

AN OPTIMIZED MULTI-STAGE SCHEME TO COORDINATE STEERING AND BRAKING*

A. TAVASOLI[1] AND M. NARAGHI[2**]

[1]Sama Technical and Vocational Training College, Islamic Azad University, Karaj Branch, Karaj, I. R. of Iran
[2]Dept of Mechanical Engineering, Amirkabir University of Technology, Tehran, I. R. of Iran
Email: naraghi@aut.ac.ir

Abstract– A novel Integrated Vehicle Dynamics Control (IVDC) scheme is presented to coordinate active steering and braking subsystems. The multi-stage coordination scheme is based on the phase-plane Method. The first stage includes the high-level controller which integrates three individual controllers according to vehicle states in the phase plane. In the next stage, an optimized scheme is established to allocate the control objectives to individual braking and steering forces. To achieve this, an inequality-constrained optimization problem, including driver's brake demand, is solved analytically. Coefficients of the cost function are adapted based on the vehicle phase-plane trajectory to realize a proper coordination of braking and steering subsystems. Simulation results validate the effectiveness of the proposed method to enhance the vehicle dynamics control.

Keywords– Coordinated, vehicle dynamics, active steering, wheel braking, optimal, tire force distribution, phase-plane method

1. INTRODUCTION

Through the last two decades, numerous active safety systems have been developed to enhance handling and stability of ground vehicles, and considerable improvements have been achieved in this regard. However, saturation of tire forces, as well as limitations in control of every aspect of vehicle dynamics in critical maneuvers keeps this area challenging and attractive to the researchers. The latest approaches to this problem include: coordinated (as well as integrated) vehicle dynamics control, and optimal distribution of tire forces.

A functional integration of slip-ratio control and active suspension for lateral vehicle dynamics was discussed in [1]. Integration of individual wheel braking and active front and rear wheel steerings was presented [2]. In another work, [3], the feedback linearization technique was applied to the problem of integrated vehicle control using steering and brakes. In 2006, Crolla suggested a rule-based integration scheme to coordinate active steering, driveline, and braking [4].

In the context of optimal distribution of tire forces, force distribution to maximize acceleration/deceleration of a four-wheel vehicle during cornering was studied in [5]. Mokhyamar and Abe [6] presented a method of tire force distribution to minimize entire tires workload usage. The notion of Adaptive-Optimal Distribution of tire Forces (AODF) was introduced by the authors in [7]. An optimizing scheme is suggested to achieve maximum handling with guaranteed vehicle dynamics stability [8]. To assure vehicle dynamics stability, the standard stability constraints of the phase-plane are incorporated into the optimal distribution of tire forces unit. To distribute vehicle control among individual tire forces constrained to nonlinear saturation condition, static and dynamic control allocation

*Received by the editors January 10, 2012; Accepted March 9, 2013.
**Corresponding author

techniques are introduced into IVDC [9], [10], and the results of both methods are compared [10]. Optimized coordination of brakes and active steering for a 4WS passenger car was considered [11].

In the present work, a multi-stage IVDC based on adaptive-optimal distribution of tire forces is considered. In a new approach, the concept of coordination based on phase-plane method has been utilized to make both consistency between high-level control objectives and the other to integrate steering and braking subsystems in an optimal way. While this method applies merits of ODF to the phase-plane approach, it contributes to the related literature in the following ways.

- The phase plane method is utilized to organize several high-level control objectives for the ODF system. In this regard, a new dynamics stability controller uses both steering and braking subsystems in an optimal manner.
- An adaptive optimal approach is established to allocate the integrated high-level control objectives to the individual steering and braking tire forces in the presence of braking demand of the driver. A new optimization problem is defined and solved analytically.
- An adaptation mechanism is considered which adjusts different weighting coefficients of the cost function in the optimization problem according to the phase-plane notion. Thus, a *phase-plane based adaptive-optimal approach* is utilized to distribute tire forces.

The effectiveness of the proposed method is evaluated through simulation results. The operation of a nonlinear vehicle model under the proposed method is examined, and by comparison with the previous results, the conclusions of the work are drawn.

The rest of the paper is organized as follows: The next section presents the high-level control design procedure. In section 3, the AODF method is demonstrated. Sections 4 and 5 are devoted to simulation results and concluding remarks.

2. COORDINATED HIGH-LEVEL CONTROL DESIGN

In general, vehicle handling and stability are achieved through controlling the yaw rate and side-slip angle, respectively. To this end, according to the vehicle lateral dynamics, there are two available virtual control inputs of total body lateral force and yaw moment. To design virtual control inputs through a coordinated high-level controller, individual high-level control laws for handling and stability are organized according to the phase-plane methodology. A description of various regions in the phase-plane of the side-slip angle, β, has been shown in Fig. 1, for reference region of stability control definition [12]. In what follows, the design procedures for different high-level control objectives are first presented. Then, a phase-plane based adaptation mechanism is proposed to coordinate several high-level control objectives.

a) Individual controllers design

In this section, three individual control laws are demonstrated. The controller design is based on a 2DOF linear vehicle model, with constant speed. The basic equations of motion for this model are [13]:

$$mV\left(\dot{\beta} + r\right) = Y \tag{1}$$

$$I_z\dot{r} = M \tag{2}$$

where m and I_z denote the total mass and yaw moment of inertia of the vehicle, respectively, V is the vehicle velocity, and r represents the yaw rate. M and Y are desired body yaw moment and lateral force. To deal with the substantial nonlinear characteristics and uncertainties of the vehicle dynamics, individual controllers based on sliding-mode methodology are designed to ensure robustness.

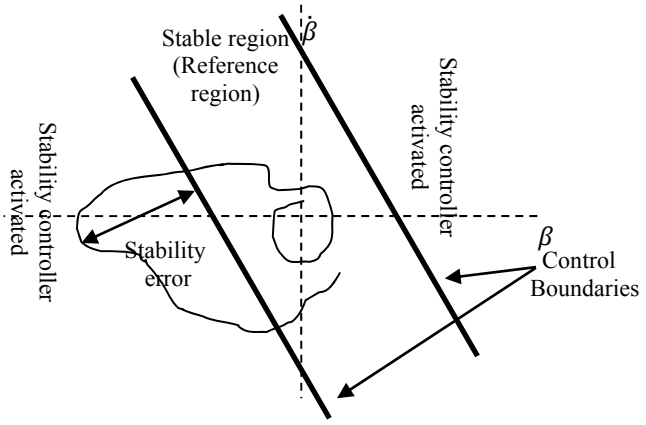

Fig. 1. Different regions in $\beta - \dot{\beta}$ phase-plane

1. Controller design for the vehicle handling: To improve vehicle manoeuvrability, generalized body lateral force and yaw moment are used to control side-slip angle and yaw rate, respectively. Design procedure is based on Eqs. (1) and (2) which represent a 2DOF linear model. A reference model [13] generates the desired yaw rate for the vehicle handling. To account for un-modelled dynamics and uncertainties, the disturbance terms, ω_β and ω_r, are embedded into each equation to get

$$mV(\dot{\beta} + r) = Y + \omega_\beta \tag{3}$$

$$I_z\dot{r} = M + \omega_r \tag{4}$$

The unknown, but bounded, disturbances could be time dependent functions of different vehicle states. To overcome the substantial uncertainties in vehicle dynamic modelling, we adopt sliding mode control that has been proven effective in achieveing a robust vehicle control design [14]. To create the total lateral force, Y, for a zero desired side-slip angle, the sliding surface is defined as:

$$s_\beta = \beta \tag{5}$$

Differentiating this equation and considering (3)

$$\dot{s}_\beta = \frac{Y}{mV} - r + \Delta_\beta \tag{6}$$

where the term $\Delta_\beta = \frac{\omega_\beta}{mV}$ is assumed to be bounded to a known value, $\bar{\Delta}_\beta$, so that

$$|\Delta_\beta| < \bar{\Delta}_\beta \tag{7}$$

To meet the sliding condition [15]

$$s_\beta \dot{s}_\beta \le -\eta_\beta |s_\beta|, \quad \eta_\beta > 0 \tag{8}$$

the desired body lateral force is considered as

$$Y = mV(r + v_\beta) \tag{9}$$

in which v_β is to be designed. Insert (9) in (6) to get the left side of (8) as

$$s_\beta \dot{s}_\beta = \beta(\Delta_\beta + v_\beta) \tag{10}$$

whose combination with (7) is given by

$$s_\beta \dot{s}_\beta \le |s_\beta||v_\beta| + |\Delta_\beta||s_\beta| \le |s_\beta||v_\beta| + \bar{\Delta}_\beta|s_\beta| \tag{11}$$

Then, to reach the desired behaviour of sliding condition (8), v_β is considered to be

$$v_\beta = -k_\beta sgn(s_\beta) \tag{12}$$

where $sgn(.)$ is the signum function, and $k_\beta > 0$ is a design parameter which is chosen as

$$k_\beta > \bar{\Delta}_\beta + \eta_\beta \tag{13}$$

Substituting (12) into (9), the desired body lateral force is attained. In practical implementation, to leave out the chattering effects of the sign switching function, it is replaced by a saturation function with a boundary layer thickness of $\Phi_\beta > 0$. Thus, the final control law becomes

$$Y = mV(r - k_\beta sat(\frac{s_\beta}{\Phi_\beta})) \tag{14}$$

In order to compute the body yaw moment, M_r, to track the desired yaw rate, r_d, an integral sliding surface is adopted

$$s_r = (r - r_d) + \lambda_r \int_0^t (r - r_d)d\tau, \quad \lambda_r > 0 \tag{15}$$

where the integral term is used to mitigate the undesirable yaw angle, or vehicle heading offset, and to ensure the desired vehicle heading. Differentiating (15), along with (4), leads to

$$\dot{s}_r = \frac{M_r}{I_z} - \dot{r}_d + \lambda_r(r - r_d) + \Delta_r, \qquad \Delta_r = \frac{\omega_r}{I_z} \tag{16}$$

The desired body yaw moment for handling can be derived in a similar way as presented before to get (14)

$$M_r = I_z(\dot{r}_d - \lambda_r(r - r_d) - k_r sat\left(\frac{s_r}{\Phi_r}\right)), \quad \Phi_r > 0 \tag{17}$$

where

$$k_r > \bar{\Delta}_r + \eta_r \tag{18}$$

with $\bar{\Delta}_r > 0$ being an upper bound for $|\Delta_r|$, and $\eta_r > 0$ the sliding surface parameter.

2. Dynamic stability control design: The Dynamic Stability Control (DSC) system employs the body yaw moment to control the side-slip angle. Usually, a *counter-steering* controller near the stability borders plus a PD control action for the braking subsystem is used to control the side-slip angle [1]-[4]. However, adopting the PD control action necessitates measurement of the side-slip angular acceleration, which is undesirable from a practical point of view. Here, a control law is designed to compute the body yaw moment directly for the side-slip angle control. Thus, a DSC law, which requires only side-sip angle and side-slip angle velocity based on sliding mode is introduced. To get the body yaw moment, M_{DSC}, for the side-slip angle control, first differentiate (3) and replace (4) for $\dot{r}$ to get

$$\ddot{\beta} = -\frac{M_{DSC}}{I_z} + \frac{\dot{F}_y}{mV} + \omega_{DSC} \tag{19}$$

In Eq. (19), since M_{DSC} is the control input to be designed, the actual value of the body lateral force, F_y, is used instead of its desired value Y. Also, ω_{DSC} represents total unknown uncertainties in achieving (19), and is bounded by the known value $\bar{\omega}_{DSC}$

$$|\omega_{DSC}| < \bar{\omega}_{DSC} \tag{20}$$

The boundaries of the reference region in Fig. 1 are defined as [4]

$$\left|\frac{1}{24}\dot{\beta} + \frac{4}{24}\beta\right| < 1 \tag{21}$$

Since the main task of DSC subsystem is to draw the vehicle phase-plane trajectory back into the stable region, whenever it exits this region, the sliding surface outside the stable regime is defined as

$$s_{DSC} = \begin{cases} \frac{1}{24}\dot{\beta} + \frac{4}{24}\beta - 1, & \frac{1}{24}\dot{\beta} + \frac{4}{24}\beta > 1 \\ \frac{1}{24}\dot{\beta} + \frac{4}{24}\beta + 1, & \frac{1}{24}\dot{\beta} + \frac{4}{24}\beta < -1 \end{cases} \tag{22}$$

To realize the sliding surface dynamics, differentiate (22) and use (19) and (3)

$$\dot{s}_{DSC} = -\frac{M_{DSC}}{24I_z} - \frac{4r}{24} + \frac{1}{24mV}(\dot{F}_y + 4F_y + 4\omega_\beta) + \frac{\omega_{DSC}}{24} \tag{23}$$

Growth of the side-slip angle saturates individual lateral tire forces outside the stable region. In such conditions, we can assume the total body lateral force is limited to the vehicle weight multiplied by the tire/road friction coefficient μ, i.e. μmg, and $\dot{F}_y$ is expected to be bounded as well. As a result, by considering (7) and (20), the total disturbance-like term on the right of (23) can be assumed to fulfill

$$\left|\frac{1}{24mV}(\dot{F}_y + 4F_y + 4\omega_\beta) + \frac{\omega_{DSC}}{24}\right| < \bar{\Delta}_{DSC}, \qquad \bar{\Delta}_{DSC} > 0 \tag{24}$$

To achieve the sliding condition, the same procedure applied before can be implemented such that

$$M_{DSC} = -4I_z\left(r - 6k_{DSC}sat\left(\frac{s_{DSC}}{\Phi_{DSC}}\right)\right), \quad \Phi_{DSC} > 0 \tag{25}$$

where

$$k_{DSC} > \bar{\Delta}_{DSC} + \eta_{DSC} \tag{26}$$

with $\eta_{DSC} > 0$ being the sliding surface parameter.

b) Coordination of high-level control objectives

The key problems to be addressed in coordinating different high-level controllers are which controllers to use in each regime, and how to make consistency between various control objectives to rule out possible conflicts. Accordingly, the control objectives need to be put in order of priority. To this end, based on the phase-plane concept, inside the stable region where tire forces are considered to have linear characteristics, for handling improvement, the total body yaw moment and lateral force, given by (14) and (17), are utilized to control yaw rate and side-slip angle, respectively. At higher side-slip angles, the high-level control objective transits from handling to stability. The vehicle stability is related directly to the side-slip motion, and this motion should be restricted to the stable region (Fig. 1). As the vehicle phase-plane trajectory approaches the reference boundaries, with growth of the side-slip angle, lateral tire forces saturate, and using exclusively the body lateral force, Eq. (14) is no longer a proper function to reduce side-slip motion. In such conditions, the notion of DSC is exploited to stabilize the vehicle, and the total yaw moment is used for stability control through DSC system (Eq. (25)). Consequently, the final body yaw moment is computed as:

$$M = n_r M_r + (1 - n_r)M_{DSC} \tag{27}$$

where n_r is the high-level adaptation gain which is adjusted according to the vehicle state in the phase-plane, as shown in Fig. 2. By this adaptation mechanism, hard switchings between several types of control objectives is avoided, and the control task transits from one to another instead. As a result, abrupt system responses that can be induced by sudden hard switching actions are excluded. The coordinated high-level control scheme can be found in Fig. 3.

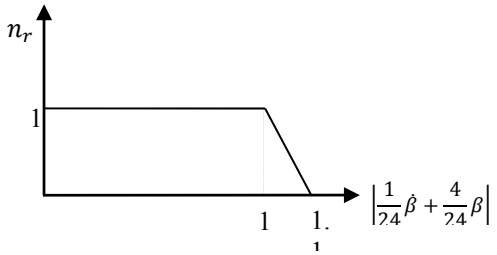

Fig. 2. Adaptation mechanism for high level control

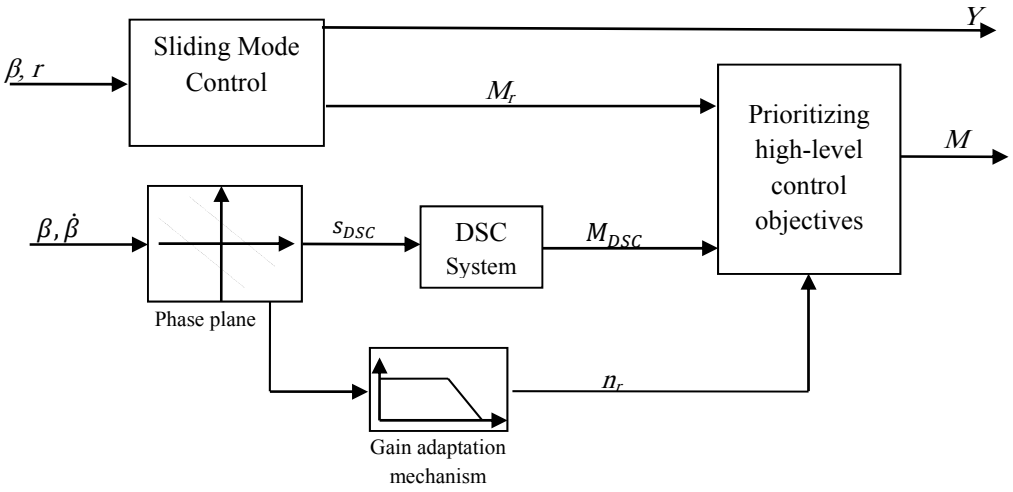

Fig. 3. Coordinated high-level control scheme

3. ADAPTIVE-OPTIMAL DISTRIBUTION OF TIRE FORCES

In this section, the notion of adaptive-optimal distribution of tire forces is used to distribute the total body force and moment of the first stage among individual tire forces. An optimization problem subjected to equality and inequality constraints is defined, and solved analytically to utilize the maximum capacity of tire forces for control objectives. The analytical solution of the inequality constrained optimization problem makes the proposed IVDC scheme more suitable for realistic applications. In order to coordinate the steering and braking subsystems, another adaptation mechanism is considered to adjust the coefficients of the cost function in this phase. Therefore, the part of the braking action that is undesirable by driver, and is used only for DSC system, *brake-based DSC*, is disabled inside the stable region of the phase-plane. Accordingly, the negative effect of the brake-based DSC on the longitudinal motion is averted in this region. Once the side-slip angle increases and vehicle goes beyond the stable regime the brake-based DSC is activated to limit the side-slip motion.

a) Formulation and solution of the constrained optimization problem

With the proposed AODF, we seek to fulfill two main goals. One is to utilize the maximum capability of tire forces and the other is to manage the active steering and braking subsystems. These are accomplished by considering and optimizing a convenient two part cost function. The first part, which is a summation of squared normalized resultant tire forces (tires workload), is to minimize tires workload and the second one, being the squared summation of normalized longitudinal tire forces, enables adjusting the steering and braking contributions in IVDC. The cost function is written according to:

$$f(\boldsymbol{X}) = \sum_{i=1}^{4}\left\{A_i\frac{F_{xi}^2+F_{yi}^2}{(\mu_i F_{zi})^2}+B_i\left(\frac{F_{xdi}}{\mu_i F_{zi}}\right)^2\right\} = \sum_{i=1}^{4}\left\{A_i\frac{(F_{xbi}+F_{xdi})^2+F_{yi}^2}{(\mu_i F_{zi})^2}+B_i\left(\frac{F_{xdi}}{\mu_i F_{zi}}\right)^2\right\} \quad (28)$$

where i denotes wheel number, F_{xi} and F_{yi} are the total longitudinal and lateral tire forces, F_{xdi} and F_{xbi} are the longitudinal braking forces due to DSC operation and driver's demand, respectively, F_{zi} is the vertical

load, and μ_i is the tire friction coefficient, all defined in the vehicle body fixed coordinate system, as shown in Fig. 4. In addition, A_i and B_i are weighting coefficients to be adjusted and $\boldsymbol{X}$ is a 12×1 vector that contains tire forces, as dependent variables for the cost function. It is assumed that each wheel can be steered independently and only braking torques at wheels are possible.

The weighting coefficient B_i is updated by means of another phase-plane based adaptation mechanism. This value determines the contribution of the braking due to the DSC system in the objective function. Thus, when the vehicle phase-plane trajectory is within the stable region, in order to prevent negative effects of braking on longitudinal dynamics and disturbances to the driver, the coefficient B_i is set to a large value (1000 in simulations). Accordingly, in this region, the contribution of braking due to DSC in the cost function is increased and this subsystem is disabled. As the side-slip dynamics moves toward unstable region of the phase-plane the coefficient B_i transits to 0, thereby decreasing the contribution of brake-based DSC in the cost function. Therefore, in this regime brake-based DSC is activated to take advantage of this system for vehicle stabilization. Additionally, to further reduce the influence of brake-based DSC on the longitudinal motion, the operation of this system is postponed by delaying the adaptation gain of the AODF relative to that of high-level control, as seen in Fig. 5. By this delay, when the vehicle stability is in question, the DSC system will first operate through steering subsystem, by applying active counter-steering, to stabilize the vehicle. However, as the lateral acceleration grows and the phase-plane curve goes further out of the stable region, the effectiveness of the steering subsystem for vehicle stabilization fades away and, hence, braking is activated. In this condition, the task of the stability control through DSC is shared between steering and braking actuation concepts by AODF system.

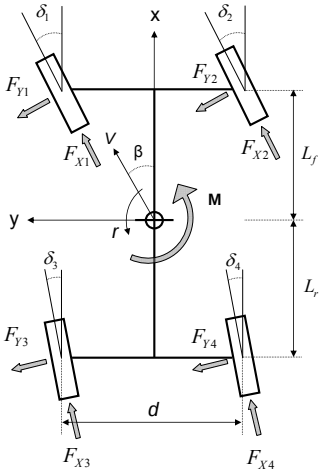

Fig. 4. Vehicle dynamics model schematic in top view

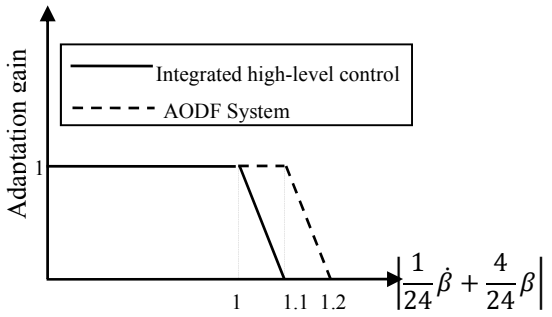

Fig. 5. Adaptation gains in different phases of IVDC

The sum of the lateral forces and yaw moments acting on the vehicle by each tire force should equal to the required total lateral force, *Y*, and yaw moment, *M*, computed based on the presented integrated high-level control. Therefore, referring to Fig. 4, all of the variables in objective function must satisfy the two equality constraints as follows:

$$Y = \sum_{i=1}^{4} F_{yi} \tag{29}$$

$$M = \sum_{i=1}^{2}\left(L_f F_{yi} - L_r F_{y(i+2)}\right) + \frac{d}{2}\sum_{i=1}^{2}\left(F_{x(2i)} - F_{x(2i-1)}\right) \tag{30}$$

In addition, the longitudinal braking forces F_{xbi} should assure the demanded total braking force, $a_x<0$, by driver

$$F_x = ma_x = \sum_{i=1}^{4} F_{xbi} \tag{31}$$

On the other hand, we assume only braking torque is possible at each wheel and the driveline torque is excluded. These words are written as

$$g_j = F_{xj} = F_{xdj} + F_{xbj} \leq 0, \qquad j = 1, \dots, 4 \tag{32}$$

Further, the statement that "the positive braking torque has no physical meaning" results in:

$$g_j = F_{xb(j-4)} \leq 0, \qquad j = 5, \dots, 8 \tag{33}$$

Thus, the cost function contains twelve variables, which must satisfy three equality constraints (29)-(31), and eight inequality constraints in (32) and (33).

It can be readily shown that the objective and constraint functions are convex. Therefore, the Karush-Kuhn-Tucker (KKT) conditions are necessary and sufficient for a global minimum [16]. In this paper, the solution of the optimization problem is simplified by developing an intuition to assess which inequality constraints may be active at each time step, according to the vehicle dynamics. In a typical optimization problem, all inequality constraints that are treated as equalities at the optimum point constitute the *active set*. The recognition of the active set is a key factor to solving any optimization problem. The inequality constraints of the active set are regarded as equalities and the remaining inequality constraints are disregarded [17]. Hence, as the active set is realized, the inequality optimization problem turns into an equality one. To find out the feasible active sets for our problem, off-line computations were performed in [18]. At each stage, a combination of g_j-s was treated as an active set and, based on this specific active set, KKT conditions were solved to get the optimization variables, i.e. individual tire forces. Then, the inequality constraints in KKT conditions were checked and only the solutions satisfying these inequalities were chosen as a feasible solution. All possible combinations of g_j-s were examined and it was concluded that, according to the sign of the body yaw moment M, only five cases might yield a true active set. The possible solutions are presented in the Appendix so that the desired tire forces can be obtained through these equations.

Then, using the inverse of simple tire model the active steering angle of each wheel, δ_i, can be determined, as depicted in [7]. Further, by ignoring the rotational dynamics of wheels, it is assumed that the applied torque at each wheel is equal to the wheel radius times the desired longitudinal force. Nonetheless, to avoid wheel lock, specifically in critical maneuvers wherein the demanded longitudinal forces by AODF might be high, an ABS for a brake by wire system is considered to compute the final braking torque, T_i, at each wheel. The overall scheme of the proposed IVDC can be seen in Fig. 6.

4. SIMULATION RESULTS

In this section, the operation of the vehicle under suggested IVDC is examined through simulations. A 9DOF nonlinear vehicle model is used for this purpose [7]. Also, a driver model, validated experimentally [19], is used to simulate the driver's behavior in different maneuvers. To compare the proposed method with previous works, we present the results of AODF with a combined high-level control, combined ODF, for which no coordination is made among high-level control objectives [6], [7], [20], and [21]. In all maneuvers, the vehicle is assumed to move with an initial velocity of 130 km/h on a slippery road where the coefficient of friction is 0.3.

a) Single-lane changing without driver's braking command

A Single-lane change (SLC) without any braking demand by driver is considered as the first maneuver. Simulation results for this scenario are shown in Figs. 7-13, wherein the results of the present work have been denoted by "Coordinated AODF". As depicted in Figs. 7-9, the vehicle with no active control and only guided by driver has an oscillatory and completely unstable response in this critical

maneuver. Nonetheless, using active safety control through AODF system, with either combined or integrated high-level controller, makes the vehicle converge to the intended path by driver. Further, the vehicle with integrated high-level control has the best performance in converging to the desired path, following the desired yaw rate, and reducing the side-lip angle. In Fig. 10, the phase-plan trajectory under Coordinated AODF has converged to the stable region more effectively due to efficient function of DSC. This approach has also kept the tires away from saturation more efficiently, as seen by Fig. 11. The plot of longitudinal forces, Fig. 12, and active steering, Fig. 13, are shown to assess how the suggested method makes use of the available actuators. Outside the reference region, Coordinated AODF has demanded braking forces at wheels on the vehicle right only in a while to stabilize the vehicle. At the same time, Combined AODF has applied more braking forces, thus increasing the negative effects of braking on the vehicle longitudinal dynamics. Further, active steering by both AODF systems is identical until the vehicle phase-plane trajectory leaves the stable region in the phase-plane. Then, Coordinated AODF has applied counter-steering to further stabilize the vehicle. Also, the active steering by Coordinated AODF is smoother and more proper.

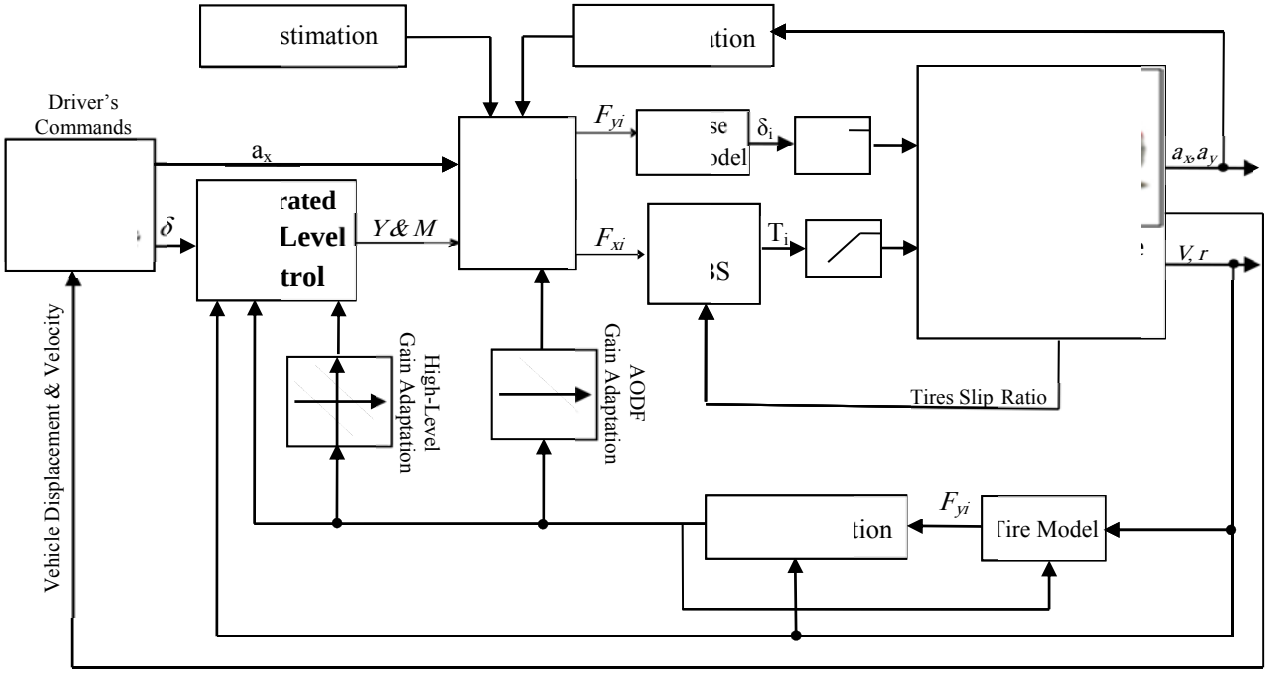

Fig. 6. Structure of the overall IVDC system

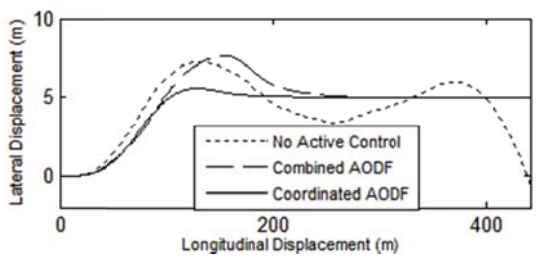

Fig. 7. Vehicle path in SLC without driver's braking

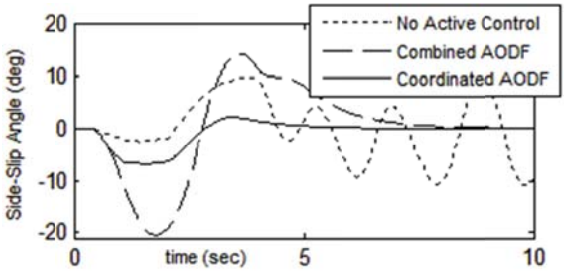

Fig. 9. Side-slip angle in SLC without driver's braking

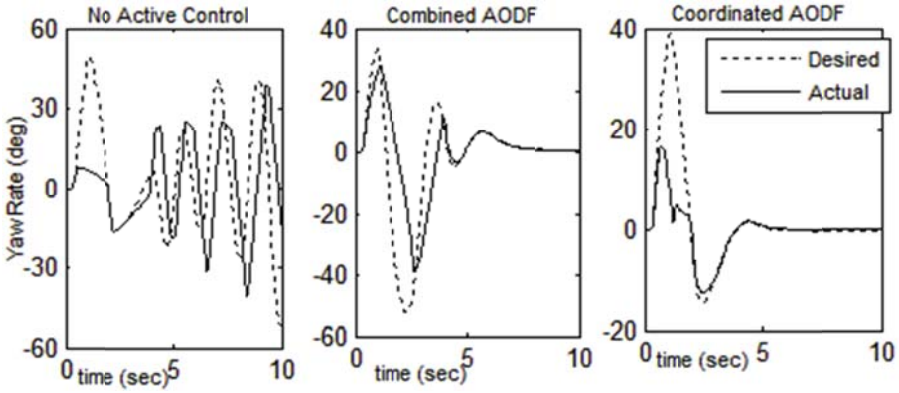

Fig. 8. Yaw rate in SLC without driver's braking

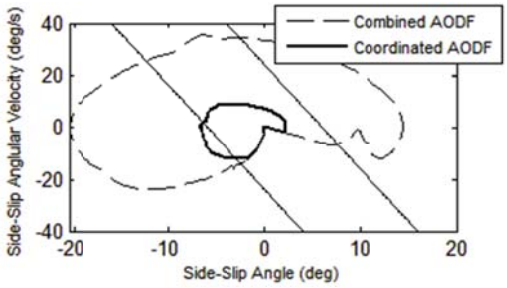

Fig. 10. Phase-plane trajectory in SLC without driver's braking

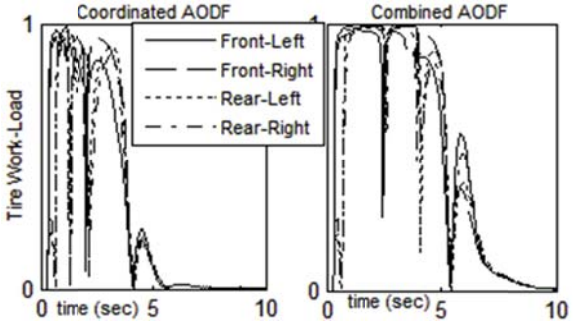

Fig. 11. Tires work-load in SLC without driver's braking

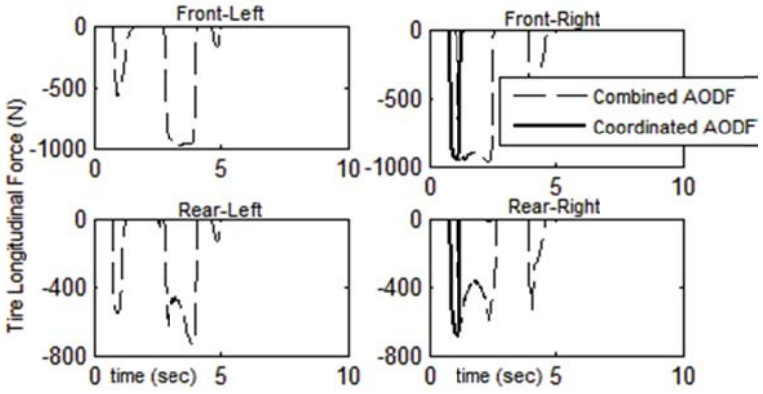

Fig. 12. Tire longitudinal forces commanded by DSC in SLC without driver's braking

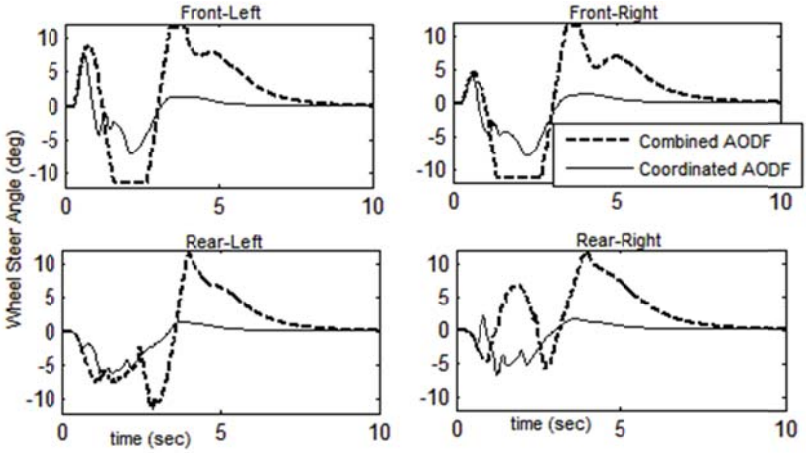

Fig. 13. Active steering in SLC without driver's braking

b) Single-lane change maneuver with driver's braking command

To examine the function of the proposed IVDC in a more critical maneuver, SLC with driver's braking demand of *-0.3g*, between *t=1s* and *t=4s*, is considered. The response of the vehicle to this maneuver is in shown in Figs. 14-18. Again it is seen that the vehicle under exclusively driver's management is compeletely unstable. On the other hand, the vehicle under Coordinated AODF has the best response in terms of vehicle path in Fig. 14, yaw rate in Fig. 15, and side-slip angle in Fig. 16. These are due to the fact that Coordinated AODF utilizes the DSC system to keep the vehicle phase-plane trajectory inside the stable region so effectively, as shown by Fig. 17. Figure 18 reveals how the Coordinated AODF distributes the yaw moment demanded by DSC among tire longitudinal forces. As vehicle phase plan trajectory leaves the stable region, the DSC system applies braking torques on right wheels to stabilize the vehicle. This braking torque, which is undesirable for passengers, has been applied only for a short period of time due to proper functioning of the proposed adaptation mechanisms. Then, as the vehicle phase plan trajectory returns to the stable area, Coordinated AODF system commands positive longitudinal forces for DSC operation to release the brakes, thereby decreasing the total tires work-load.

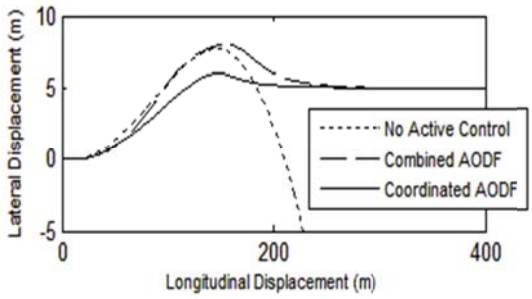

Fig. 14. Vehicle path in SLC with driver's braking

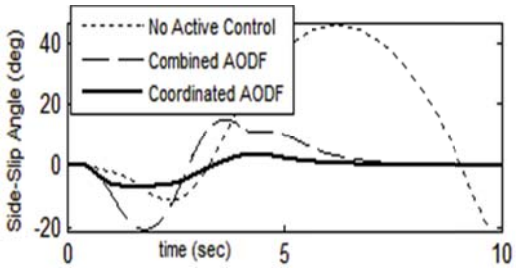

Fig. 16. Side-slip angle in SLC with driver's braking

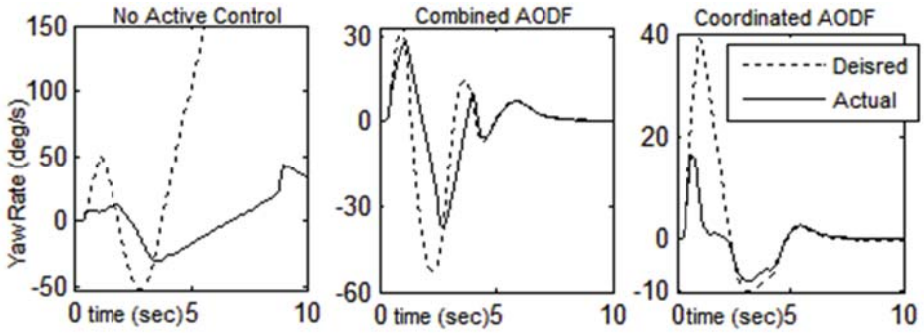

Fig. 15. Yaw rate in SLC with driver's braking

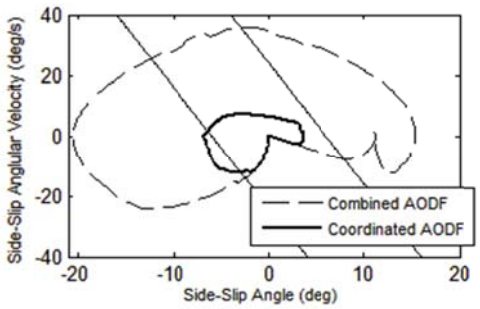

Fig. 17. Phase-plane trajectory in SLC with driver's braking

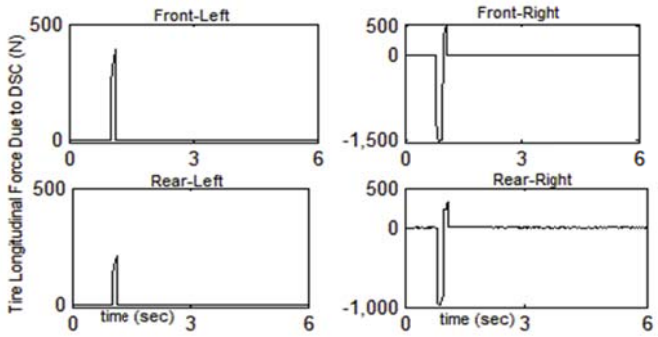

Fig. 18. Longitudinal forces by DSC in SLC with driver's braking

5. CONCLUSION

Optimal integration of active steering and braking subsystems was presented in this paper. A coordinated high-level controller averts possible conflicts between various control objectives. A new DSC was designed and by the proposed method the DSC exploits both active steering and braking actuations for vehicle control in an optimal manner. Then, the the high-level control is distributed over the individual tire forces through an adaptive-optimal approach in the presence of driver's braking acceleration demand. So, the maximum capacity of tire forces is used to fulfill the control objectives. At the same time, the active steering and braking subsystems are coordinated through another phase-plane based adaptation mechanism. To this end, the weighting coefficients of the cost function are adjusted based on the phase-plane method. An analytical solution was derived for the proposed optimization problem. The vehicle behavior under the proposed method was investigated during some critical maneuvers and the results were compared with those of earlier work. It is concluded that under the proposed scheme the vehicle stability is enhanced significanly compared to previous works of the literature.

REFERENCES

1. Smakman, H. T. (2000). Functional integration of slip control with active suspension for improved lateral vehicle dynamics. *PhD Dissertation.* s.l. : Delft University of Technology, The Netherlands.
2. Selby, M. (2003). Intelligent vehicle motion control. Leeds : PhD Dissertation, University of Leeds, UK.
3. Burgio, G. & Zegelaar, P. (2006). *Integrated vehicle control using steering and brakes*. *International Journal of Control*, Vol. 79, No. 5, pp. 534–541.
4. He, J. (2006). Coordination of active steering, driveline, and braking for integrated vehicle dynamics control. *Proc. IMechE*, Vol. 220, Part D: J. Automobile Engineering, pp. 1401-1421.
5. Peng, H. & Hu, J. S. (1999). Traction/braking force distribution for optimal longitudinal motion during curve following. *Vehicle System Dynamics*, Vol. 26, No.4, pp. 301-320.
6. Mokhyamar, O & Abe, M. (2004). Simultaneous optimal distribution of lateral tire forces for the model following control. *Journal of Dynamic system, Measurement, and Control*, Vol. 126, pp. 753-763.
7. Naraghi, M., Roshanbin, A. & Tavasoli, A. (2010). Vehicle stability enhancement – an adaptive optimal approach to the distribution of tyre forces. *Proc. IMechE, Part D: J. Automobile Engineering*, Vol. 224, pp. 443-453.
8. Tavasoli, A. & Naraghi, M. (2011). An optimizing scheme to achieve maximum handling with guaranteed vehicle dynamics stability. *Australian Journal of Basic and Applied Sciences*, Vol. 5, No. 11, pp. 1989-2001.
9. Tavasoli, A. & Naraghi, M. (2013). Interior point method to optimize tire force allocation in 4-wheeled vehicles using high-level sliding mode control with adaptive gain. *Asian Journal of Control*, Vol. 15, No. 4, pp. 1188–1200.

10. Tavasoli, A. & Naraghi, M. (2012). Vehicle sliding mode control with adaptive upper bounds: static versus dynamic allocation to saturated tire forces. *Mathematical Problems in Engineering*, Vol. 2012, pp. 1-31.
11. Tavasoli, A. & Naraghi, M. (2012). Optimized coordination of brakes and active steering for a 4WS passenger car. *ISA Transactions*, Vol. 51, pp. 573–583.
12. Inagaki, S., Kshiro, I. & Yamamoto, M. (1994). Analysis on vehicle stability in critical cornering using phase-plane method. *AVEC '94*. pp. 287-292.
13. Rajamani, R. (2006). *Vehicle dynamics and control*. New York : Springer Science.
14. Guclu, R. & Yagiz, N. (2004). Comparison of different control strategies on a vehicle using sliding mode control. *Iranian Journal of Science & Technology, Transaction B, Engineering*, Vol. 28, No. B4, pp. 413-422.
15. Khalil, H. K. (2002). *Nonlinear systems*. 3rd ed: Prentice Hall.
16. Boyd, S. & Vandenberghe, L. (2009). *Convex optimization*. 7th Ed, Cambridge University Press.
17. Nocedal, J. & Wright, S. J. (2006). *Numerical optimization*. 2nd Ed, Springer Science, USA.
18. Roshanbin, A. (2008). *Vehicle stability enhancement- an adaptive-optimal approach to distribution of tire forces*. Iran- Tehran, Amirkabir University of Technology.
19. Abe, M. (2009). *Vehicle handling dynamics: theory and application*. Elsevier Ltd, UK.
20. Wang, J. & Longoria, R. G. (2009). Coordinated and reconfigurable vehicle dynamics control. *IEEE Transactions on Control Systems Technology*, Vol. 17, No. 3, pp. 723-732.
21. Tjønnås, J. & Johansen, T. A. (2010). *Stabilization of automotive vehicles using active steering and adaptive brake control allocation*. *IEEE Transactions on Control Systems Technology*, Vol. 18, No 3, pp. 545-558.
22. Allen, R. W., Rosenthal, T. J. & Szostak, H. T. (1988). Steady state and transient analysis of ground vehicle handling. SAE paper, No 870495, pp. 482-512, 1988.

APPENDIX: POSSIBLE SOLUTIONS OF KKT CONDITIONS

The optimization problem in Section 3 is summarized as

$$\begin{aligned} &minimize && f(\boldsymbol{X}) = \sum_{i=1}^{4}\left\{A_i \frac{(F_{xbi}+F_{xdi})^2+F_{yi}^2}{(\mu_i F_{zi})^2} + B_i\left(\frac{F_{xdi}}{\mu_i F_{zi}}\right)^2\right\} \\ &subject\ to\ equalities && \begin{cases} e_1 = Y - \sum_{i=1}^{4} F_{yi} = 0 \\ e_2 = M - \sum_{i=1}^{2}\left(L_f F_{yi} - L_r F_{y(i+2)}\right) + \frac{d}{2}\sum_{i=1}^{2}\left(F_{x(2i)} - F_{x(2i-1)}\right) = 0 \\ e_3 = F_x - ma_x = \sum_{i=1}^{4} F_{xbi} = 0 \end{cases} \\ &and\ inequalties && g_j \le 0, \quad j = 1,\dots,8 \end{aligned}$$

The vector of desired individual tire forces is defined as

$$\boldsymbol{u} = \left[F_{xd1}, F_{xd2}, F_{xd3}, F_{xd4}, F_{xb1}, F_{xb2}, F_{xb3}, F_{xb4}, F_{y1}, F_{y2}, F_{y3}, F_{y4}\right]$$

To realize $\boldsymbol{u}$, KKT conditions [16] are applied to the optimization problem and the following equations are derived

$$\begin{cases} \dfrac{\partial f}{\partial \boldsymbol{u}} + \sum_{i=1}^{3} \lambda_{e_i} \dfrac{\partial e_i}{\partial \boldsymbol{u}} + \sum_{j=1}^{8} \lambda_j \dfrac{\partial g_j}{\partial \boldsymbol{u}} = \boldsymbol{0} \\ e_i = 0, \quad i = 1,\dots,3 \\ \lambda_j g_j = 0, \quad j = 1,\dots,8 \\ g_j \le 0 \\ \lambda_j \ge 0 \end{cases}$$

in which λ_{e_i} and λ_j are the Lagrange multipliers corresponding to equality and inequality constraints respectively. Then, KKT conditions result in these five sets of linear equations as follows [18]:

1- If $\lambda_{1,3,5,7} = 0, \quad \lambda_{2,4,6,8} \ge 0, \quad g_{1,3,5,7} \le 0, \quad g_{2,4,6,8} = 0,$ then $[\mathbf{A}^{(1)}]_{13\times13}\ \mathbf{x}^{(1)}_{13\times1} = \mathbf{b}^{(1)}_{13\times1}$ where

$$\mathbf{x}^{(1)} = [F_{xd1} \quad F_{xd2} \quad F_{xd3} \quad F_{xb1} \quad F_{xb2} \quad F_{xb3} \quad F_{y1} \quad F_{y2} \quad F_{y3} \quad \lambda_2 \quad \lambda_4 \quad \lambda_6 \quad \lambda_8]^T$$

2- If $\lambda_{1,3,5,7} \geq 0$, $\lambda_{2,4,6,8} = 0$, $g_{1,3,5,7} = 0$, $g_{2,4,6,8} \leq 0$, then $[\mathbf{A}^{(2)}]_{13\times13}\ \mathbf{x}^{(2)}_{13\times1} = \mathbf{b}^{(2)}_{13\times1}$ where

$$\mathbf{x}^{(2)} = [F_{xd1} \quad F_{xd2} \quad F_{xd3} \quad F_{xb1} \quad F_{xb2} \quad F_{xb3} \quad F_{y1} \quad F_{y2} \quad F_{y3} \quad \lambda_1 \quad \lambda_3 \quad \lambda_5 \quad \lambda_7]^T$$

3- If $\lambda_{1,3,5,6,7,8} = 0$, $\lambda_{2,4} \geq 0$, $g_{1,3,5,6,7,8} \leq 0$, $g_{2,4} = 0$, then $[\mathbf{A}^{(3)}]_{11\times11}\ \mathbf{x}^{(3)}_{11\times1} = \mathbf{b}^{(3)}_{11\times1}$ where

$$\mathbf{x}^{(3)} = [F_{xd1} \quad F_{xd2} \quad F_{xd3} \quad F_{xb1} \quad F_{xb2} \quad F_{xb3} \quad F_{y1} \quad F_{y2} \quad F_{y3} \quad \lambda_2 \quad \lambda_4]^T$$

4- If $\lambda_{2,4,5,6,7,8} = 0$, $\lambda_{1,3} \geq 0$, $g_{2,4,5,6,7,8} \leq 0$, $g_{1,3} = 0$, then $[\mathbf{A}^{(4)}]_{11\times11}\ \mathbf{x}^{(4)}_{11\times1} = \mathbf{b}^{(4)}_{11\times1}$ where

$$\mathbf{x}^{(4)} = [F_{xd1} \quad F_{xd2} \quad F_{xd3} \quad F_{xb1} \quad F_{xb2} \quad F_{xb3} \quad F_{y1} \quad F_{y2} \quad F_{y3} \quad \lambda_1 \quad \lambda_3]^T$$

5- If $\lambda_j = 0$, $g_j \leq 0$, $j = 1,...,8$ then $[\mathbf{A}^{(5)}]_{9\times9}\ \mathbf{x}^{(5)}_{9\times1} = \mathbf{b}^{(5)}_{9\times1}$ where

$$\mathbf{x}^{(5)} = [F_{xd1} \quad F_{xd2} \quad F_{xd3} \quad F_{xb1} \quad F_{xb2} \quad F_{xb3} \quad F_{y1} \quad F_{y2} \quad F_{y3}]^T$$

The elements of the matrices, $[\mathbf{A}^{(\mathbf{n})}]$ and $\boldsymbol{b}^{(\boldsymbol{n})}$, $n = 1, \ldots, 5$, are the functions of A_i, B_i, μ_i, F_{zi}, d, L_f, L_r, F_y, and M.